Available online at www.sciencedirect.com
SCIENCE DIRECT
Journal of Power Sources 157 (2006) 657–665
JOURNAL OF POWER SOURCES
www.elsevier.com/locate/jpowsour

Direct ethanol fuel cell anode simulation model

George Andreadis, Shuqin Song, Panagiotis Tsiakaras *

Department of Mechanical and Industrial Engineering, School of Engineering, University of Thessaly, Pedion Areos, 383 34, Greece

Received 30 September 2005; accepted 16 December 2005
Available online 9 February 2006

Abstract

The electrochemical behavior of a *direct ethanol feed proton exchange membrane fuel cell* (DEFC) operating under steady-state isothermal conditions at 1 atm at both anode and cathode sides is considered. A mathematical model that describes in one phase and one dimension the ethanol mass transport throughout the anode compartment and proton exchange membrane is developed. The influence of the operation parameters such as current density, temperature, catalyst layer thickness and ethanol feed concentration on both anode overpotential and ethanol crossover rate has been examined. According to the simulation results, it was found that the anode overpotential is more sensitive to the protonic conductivity than to the diffusion coefficient of ethanol in the catalyst layer. It was concluded that in the case of low current density values and high concentrations of ethanol aqueous solutions, ethanol crossover is a serious problem for a DEFC performance. Finally, it was found a good agreement between simulation and experimental results.

Keywords: Mathematical modeling; Direct ethanol fuel cell (DEFC); Ethanol crossover

1. Introduction

The last decade *direct ethanol fuel cells* (DEFCs) have attracted more and more interest due to ethanol intrinsic advantages [1–21]. It has already been recognized that ethanol is a promising fuel which is non-toxic, renewable, and can be easily produced in great quantity by the fermentation of sugar-containing raw materials [1,2]. Moreover, a high theoretical mass energy density (about 8.00 kWh kg^{-1}) [16] provides it with a potential candidate fuel for proton exchange membrane fuel cells. However, there are some challenges that DEFCs meet, such as the high anode overpotential values, slow ethanol electro-oxidation kinetic and fuel crossover from the anode to cathode through the membrane, which inevitably decrease the fuel cell efficiency. At the same time, the permeated ethanol and its oxidation intermediate products could poison the cathode catalyst. In our previous work the experimental results of ethanol crossover have already been reported [9].

Mathematical modeling is essential for the development of fuel cells because it allows extensive comprehension of the parameters affecting the performance of a single fuel cell or fuel cell systems [23–26]. The work of Haraldsson and Wipke [3] is directed to the analysis and evaluation of fuel cell system models. Jeng and Chen [12] developed a mathematical model in order to predict the behavior of a direct methanol fuel cell and examine the effect of the current density on methanol crossover. However, there are some empirical models [8] developed specifically for various applications and operating conditions.

In the present work, a mathematical model for the simulation of a direct ethanol fuel cell anode has been developed with the purpose to further investigate the effect of fuel cell main parameters (current density, temperature, ethanol concentration) on both ethanol crossover and anode overpotential. More precisely, this model aims at the solution of the governing equations of mass transport through both the catalyst layer and the proton exchange membrane.

2. Theory

As schematically shown in Fig. 1, the ethanol fed to the anode compartment of a direct ethanol fuel cell could be partially reacted, partially unreacted and as the experimental results [9,10] showed, partially crossovered to the cathode compartment. It can also be seen that the anode compartment consists of diffusion layer and catalyst layer. The diffusion layer is made of

* Corresponding author. Tel.: +30 24210 74065; fax: +30 24210 74050.
E-mail address: tsiak@mie.uth.gr (P. Tsiakaras).

0378-7753/$ – see front matter © 2006 Elsevier B.V. All rights reserved.
doi:10.1016/j.jpowsour.2005.12.040

Nomenclature

A_v	electrode area where the reaction takes place
C_{EtOH}	local ethanol concentration
C^{an}_{EtOH}	ethanol concentration on the anode side (M)
C^{cath}_{EtOH}	ethanol concentration on the cathode side (M)
$C_{F,EtOH}$	feed ethanol concentration (M)
C^{ref}_{EtOH}	reference ethanol concentration (M)
$C_{s,EtOH}$	ethanol concentration at the surface of diffusion layer (M)
C^{0}_{EtOH}	ethanol concentration at $z = 0$ (M)
$D^{d,eff}_{EtOH}$	effective diffusion coefficient at the diffusion layer ($cm^2\ s^{-1}$)
$D^{c,eff}_{EtOH}$	effective diffusion coefficient at the catalyst layer ($cm^2\ s^{-1}$)
$D_{d,EtOH}$	diffusion coefficient of ethanol in water ($cm^2\ s^{-1}$)
D^{m}_{EtOH}	diffusion coefficient of ethanol in PEM ($cm^2\ s^{-1}$)
$D^{m}_{H_2O}$	diffusion coefficient of water in PEM ($cm^2\ s^{-1}$)
F	Faraday constant (96498 C mol^{-1})
i	protonic current density (A cm^{-2})
$i_{o,ref}$	reference exchange current density (A cm^{-2})
I	cell current density (A cm^{-2})
k_g	mass transfer coefficient of ethanol from the feed stream to diffusion layer (cm s^{-1})
k^d	mass transfer coefficient of ethanol in diffusion layer (cm s^{-1})
k^m	mass transfer coefficient of ethanol in PEM (cm s^{-1})
K_m	protonic conductivity of ionomer
K^{eff}_m	effective protonic conductivity in catalyst layer
K^{eff}_s	effective conductivity of solid phase in catalyst layer
K_S	electronic conductivity of solid phase (Pt-Ru/C) (S cm^{-1})
l_c	thickness of catalyst layer (cm)
l_d	thickness of diffusion layer (cm)
l_m	PEM thickness (cm)
M_{H_2O}	molecular weight of water (g mol^{-1})
N_{EtOH}	local ethanol flux in catalyst layer (mol $cm^{-2}\ s^{-1}$)
N^{d}_{EtOH}	ethanol flux through the diffusion layer (mol $cm^{-2}\ s^{-1}$)
N^{m}_{EtOH}	ethanol flux through PEM (mol $cm^2\ s^{-1}$)
N_{diff}	water flux due to the diffusion mechanism in PEM (mol $cm^{-2}\ s^{-1}$)
$N_{electr\ drag}$	water flux due to the electro-osmotic drag in PEM (mol $cm^{-2}\ s^{-1}$)
N_{H_2O}	local water flux in catalyst layer (mol $cm^{-2}\ s^{-1}$)
N_{d,H_2O}	water flux through the diffusion layer (mol $cm^{-2}\ s^{-1}$)
$N^{m}_{H_2O}$	water flux through PEM (mol $cm^{-2}\ s^{-1}$)
N_T	total flux of water and ethanol in catalyst layer (mol $cm^{-2}\ s^{-1}$)
R	universal gas constant (8.3144 J $mol^{-1}\ K^{-1}$)
T	cell temperature (K)
v^d	superficial velocity of water in diffusion layer (cm s^{-1})
v^m	superficial velocity of water in PEM (cm s^{-1})
y_{EtOH}	mole fraction of ethanol

Greek letters

α_a	anode transfer coefficient
ε^d	void fraction of diffusion layer
ε^c	void fraction of catalyst layer
γ	order of reaction
η	anode overpotential (V)
φ_m	potential of the ionomer phase (V)
φ_s	potential of electronic conduction phase (V)
λ_{H_2O}	electro-osmotic drag coefficient of water
ρ_{H_2O}	density of water (1.0 g cm^{-3})

a porous and electrically conductive material, through which the electrons generated in the anode catalyst layer are transported to the current collector. On the other hand, the catalyst layer is the place where the reaction of the ethanol electro-oxidation takes place, releasing protons and electrons. Both protons and electrons are then transported to the cathode: the electrons through an external circuit while the protons through a *proton exchange membrane* (PEM).

The mathematical model has been developed taking into consideration the following assumptions: (a) the cell operates under steady-state isothermal conditions, (b) the pressure in both anode and cathode compartment is 1 atm, (c) the model equations are defined in one dimesion and (d) the origin is set at the interface between the diffusion layer and the catalyst layer.

2.1. Flow channel

The ethanol concentration, which is fed into the flow channel, is indicated as feed concentration ($C_{F,EtOH}$). The ethanol transportation from the feed stream to the diffusion layer can be described by the following equation:

$$N^{d}_{EtOH} = k_g(C_{F,EtOH} - C_{s,EtOH}) \quad (1)$$

where N^{d}_{EtOH} stands for ethanol flux through diffusion layer, $C_{F,EtOH}$ ethanol feed concentration, $C_{s,EtOH}$ ethanol concentration at the surface of the diffusion layer, and k_g mass transfer coefficient. The mass transfer coefficient from the feed stream to the diffusion layer can be approximately expressed by using the empirical equation [12]:

$$k_g = 1.87 \times 10^{-4}\left(\frac{I}{0.003}\right)^{0.32} \quad (2)$$

where I denotes the current density of the fuel cell.

2.2. Diffusion layer

Diffusion layer is made of carbon particles that are inactive to the electrochemical reaction for a DEFC. After passing through

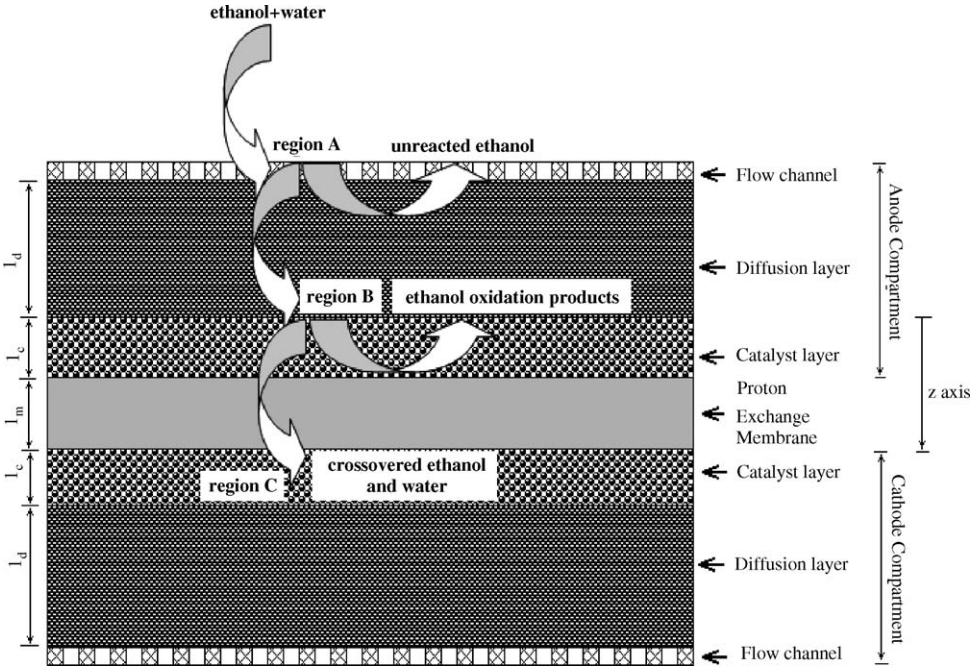

Fig. 1. Schematic presentation of a DEFC and ethanol transportation through anode compartment and PEM.

diffusion layer, water is partially consumed in the electrochemical reaction which takes place in the catalyst layer. The remaining quantity could further migrate through PEM by diffusion, electro-osmosis and hydraulic permeation. The electro-osmotic drag appears when the electrochemical cell operates, while the hydraulic permeation appears in the presence of pressure difference between anode and cathode. As above mentioned the pressure has been assumed at both anode and cathode sides equal to 1 atm and consequently the water flux through the diffusion layer can be attributed to both diffusion and electro-osmosis phenomena and described by the following equation:

$$N_{\mathrm{d,H_2O}} = \frac{I}{12F} + N^{\mathrm{m}}_{\mathrm{H_2O}} \tag{3}$$

where F is the Faraday constant and $N^{\mathrm{m}}_{\mathrm{H_2O}}$ the water flux through PEM.

Through the diffusion layer ethanol is transported by diffusion and convection:

$$N^{\mathrm{d}}_{\mathrm{EtOH}} = -D^{\mathrm{d,eff}}_{\mathrm{EtOH}} \frac{\mathrm{d}C_{\mathrm{EtOH}}}{\mathrm{d}z} + y_{\mathrm{C,EtOH}}\, N_{\mathrm{T}} \tag{4}$$

where $D^{\mathrm{d,eff}}_{\mathrm{EtOH}}$ is the effective diffusion coefficient of ethanol in the diffusion layer, $y_{\mathrm{C,EtOH}}$ the local mole fraction of ethanol in the diffusion layer, and N_{T} the total flux of ethanol and water. The effective diffusion coefficient through a porous media, the bulk diffusion coefficient ($D_{\mathrm{d,EtOH}}$) and the void fraction of the diffusion layer (ε^{d}) are related by Bruggeman's empirical equation [19,20].

$$D^{\mathrm{d,eff}}_{\mathrm{EtOH}} = (\varepsilon^{\mathrm{d}})^{3/2} D_{\mathrm{d,EtOH}} \tag{5}$$

The local mole fraction of ethanol $y_{\mathrm{C,EtOH}}$ is given as follows:

$$y_{\mathrm{C,EtOH}} = \frac{C_{\mathrm{EtOH}}}{C_{\mathrm{H_2O}} + C_{\mathrm{EtOH}}} = \frac{C_{\mathrm{EtOH}}}{C_{\mathrm{H_2O}}} = \frac{M_{\mathrm{H_2O}} C_{\mathrm{EtOH}}}{\rho_{\mathrm{H_2O}}} \tag{6}$$

Combining Eqs. (6) and (4), Eq. (4) can be expressed by a first order differential equation as follows:

$$N^{\mathrm{d}}_{\mathrm{EtOH}} = -D^{\mathrm{d,eff}}_{\mathrm{EtOH}} \frac{\mathrm{d}C_{\mathrm{EtOH}}}{\mathrm{d}z} + \frac{M_{\mathrm{H_2O}} C_{\mathrm{EtOH}}}{\rho_{\mathrm{H_2O}}} N_{\mathrm{d,H_2O}} \tag{7}$$

Assuming that $D^{\mathrm{d,eff}}_{\mathrm{EtOH}}$ and $\rho_{\mathrm{H_2O}}$ are constant, Eq. (7) can be solved within the interval of $-l_{\mathrm{d}} \le z \le 0$ taking the following form:

$$N^{\mathrm{d}}_{\mathrm{EtOH}} = \frac{C_{\mathrm{s,EtOH}} \mathrm{e}^{v^{\mathrm{d}}/k^{\mathrm{d}}} - C^{0}_{\mathrm{EtOH}}}{\mathrm{e}^{v^{\mathrm{d}}/k^{\mathrm{d}}} - 1} v^{\mathrm{d}} \tag{8}$$

where $k^{\mathrm{d}} = D^{\mathrm{d,eff}}_{\mathrm{EtOH}}/l_{\mathrm{d}}$ is the mass transfer coefficient in the diffusion layer, C^{0}_{EtOH} the ethanol concentration at the interface between the diffusion layer and the catalyst layer (i.e. at $z=0$). $v^{\mathrm{d}} = M_{\mathrm{H_2O}}\, N_{\mathrm{H_2O}}/\rho_{\mathrm{H_2O}}$ denotes the superficial velocity of water in the diffusion layer and l_{d} the thickness of the diffusion layer.

By combining Eqs. (1) and (8) and eliminating $C_{\mathrm{s,EtOH}}$, the expression of the ethanol flux through the diffusion layer as a function of the ethanol feed concentration ($C_{\mathrm{F,EtOH}}$) can be obtained:

$$N^{\mathrm{d}}_{\mathrm{EtOH}} = \frac{C_{F,\mathrm{EtOH}} \mathrm{e}^{v^{\mathrm{d}}/k^{\mathrm{d}}} - C^{0}_{\mathrm{EtOH}}}{\mathrm{e}^{v^{\mathrm{d}}/k^{\mathrm{d}}}[(v^{\mathrm{d}}/k^{\mathrm{d}}) + 1] - 1} v^{\mathrm{d}} \tag{9}$$

2.3. Catalyst layer

Catalyst layer is the place where the reaction of ethanol electro-oxidation takes place. The rate of the electrochemical

reaction can be described by using the Butler–Volmer equation and in a simpler way by the Tafel equation:

$$\frac{\mathrm{d}i}{\mathrm{d}z} = A_v i_{\mathrm{o,ref}} \left(\frac{C_{\mathrm{EtOH}}}{C_{\mathrm{EtOH}}^{\mathrm{ref}}} \right)^{\gamma} \exp\left(\frac{12\alpha_{\mathrm{a}} F\eta}{RT} \right) \tag{10}$$

where i is the local protonic current density, A_v the specific area of the reaction surface, $i_{\mathrm{o,ref}}$ the reference exchange current density, γ the order of reaction, C_{EtOH} the local ethanol concentration in the catalyst layer, $C_{\mathrm{EtOH}}^{\mathrm{ref}}$ the reference ethanol concentration, which is associated with $i_{\mathrm{o,ref}}$, α_{a} the anode charge transfer coefficient and η is the anode overpotential.

The driving force for both water and ethanol transportation through the catalyst layer consists of the diffusion and the electro-osmotic drag.

$$N_{\mathrm{EtOH}} = -D_{\mathrm{EtOH}}^{\mathrm{c,eff}} \frac{\mathrm{d}C_{\mathrm{EtOH}}}{\mathrm{d}z} + \frac{M_{\mathrm{H_2O}} C_{\mathrm{EtOH}}}{\rho_{\mathrm{H_2O}}} N_{\mathrm{H_2O}} \tag{11}$$

where $D_{\mathrm{EtOH}}^{\mathrm{c,eff}}$ is the effective diffusion coefficient of ethanol in the catalyst layer, and $N_{\mathrm{H_2O}}$ is the local water flux. The water mass balance gives:

$$N_{\mathrm{H_2O}} = \frac{I - i}{12F} + N_{\mathrm{H_2O}}^{\mathrm{m}} \tag{12}$$

where $N_{\mathrm{H_2O}}^{\mathrm{m}}$ is the water flux through PEM.

As the ethanol moves along the catalyst layer, its flux decreases due to ethanol electro-oxidation on the catalytic sites. Thus, the material balance equation for ethanol is derived from the following equation:

$$\frac{\mathrm{d}N_{\mathrm{EtOH}}}{\mathrm{d}z} = -\frac{1}{12F} \frac{\mathrm{d}i}{\mathrm{d}z} \tag{13}$$

The anode overpotential at any location within the catalyst layer is defined as:

$$\eta(z) = \varphi_{\mathrm{s}}(z) - \varphi_{\mathrm{m}}(z) \tag{14}$$

where $\varphi_{\mathrm{s}}(z)$ is the potential of the electronic conduction phase of the catalyst layer and $\varphi_{\mathrm{m}}(z)$ denotes the potential of the ionomer phase. Both $\varphi_{\mathrm{s}}(z)$ and $\varphi_{\mathrm{m}}(z)$ decrease in the z-direction, and Ohm law equation for each phase can be written as:

$$\frac{\mathrm{d}\varphi_{\mathrm{s}}}{\mathrm{d}z} = -\frac{1}{K_{\mathrm{s}}^{\mathrm{eff}}} (I - i) \tag{15}$$

$$\frac{\mathrm{d}\varphi_{\mathrm{m}}}{\mathrm{d}z} = -\frac{1}{K_{\mathrm{m}}^{\mathrm{eff}}} i \tag{16}$$

where $K_{\mathrm{s}}^{\mathrm{eff}}$ and $K_{\mathrm{m}}^{\mathrm{eff}}$ denote the effective conductivity of the solid phase and the ionomer phase, respectively. Consequently, the variation of the anode overpotential in the catalyst layer is given by the following equation:

$$\frac{\mathrm{d}\eta}{\mathrm{d}z} = \left(\frac{1}{K_{\mathrm{m}}^{\mathrm{eff}}} + \frac{1}{K_{\mathrm{s}}^{\mathrm{eff}}} \right) i - \frac{1}{K_{\mathrm{s}}^{\mathrm{eff}}} I \tag{17}$$

2.4. Proton exchange membrane

The transportation of water through PEM is the result of the combination of the following phenomena: electro-osmosis, diffusion and hydraulic permeation. However, it was assumed above that the pressure at both anode and cathode sides is equal to 1 atm. Therefore, only the effects of electro-osmosis and diffusion are considered:

$$N_{\mathrm{H_2O}}^{\mathrm{m}} = N_{\mathrm{electr\,drag}} + N_{\mathrm{diff}} \tag{18}$$

where $N_{\mathrm{electr\,drag}}$ denotes the water flux caused by the electro-osmotic drag, which at a constant cell temperature, is proportional to the cell current density I and it can be expressed as:

$$N_{\mathrm{electr\,drag}} = \lambda_{\mathrm{H_2O}} \frac{I}{F} \tag{19}$$

where $\lambda_{\mathrm{H_2O}}$ is the electro-osmotic drag coefficient of water. N_{diff} is deduced from the water concentration gradient through PEM and it can be expressed:

$$N_{\mathrm{diff}} = D_{\mathrm{H_2O}}^{\mathrm{m}} \frac{C_{\mathrm{H_2O}}^{\mathrm{an}} - C_{\mathrm{H_2O}}^{\mathrm{cath}}}{l_{\mathrm{m}}} \tag{20}$$

where $D_{\mathrm{H_2O}}^{\mathrm{m}}$ stands for the diffusion coefficient of water in PEM, l_{m} PEM thickness, $C_{\mathrm{H_2O}}^{\mathrm{an}}$ and $C_{\mathrm{H_2O}}^{\mathrm{cath}}$ the water concentration at the anode and the cathode side, respectively.

For the sake of simplicity, based on the assumption that both anode and cathode are fully hydrated, the water transportation through the membrane can be reduced into the next equation:

$$N_{\mathrm{H_2O}}^{\mathrm{m}} \cong \lambda_{\mathrm{H_2O}} \frac{I}{F} \tag{21}$$

Thus, the ethanol flux through PEM can be expressed as follows:

$$N_{\mathrm{EtOH}}^{\mathrm{m}} = \frac{C_{\mathrm{EtOH}}^{\mathrm{an}} \mathrm{e}^{v^{\mathrm{m}}/k^{\mathrm{m}}} - C_{\mathrm{EtOH}}^{\mathrm{cath}}}{\mathrm{e}^{v^{\mathrm{m}}/k^{\mathrm{m}}} - 1} v^{\mathrm{m}} \tag{22}$$

where $k^{\mathrm{m}} = D_{\mathrm{EtOH}}^{\mathrm{m}}/l_{\mathrm{m}}$ is the mass transfer coefficient of ethanol in PEM, $C_{\mathrm{EtOH}}^{\mathrm{an}}$ and $C_{\mathrm{EtOH}}^{\mathrm{cath}}$ the respective ethanol concentration at the anode and the cathode sides of PEM and $v^{\mathrm{m}} = M_{\mathrm{H_2O}} N_{\mathrm{H_2O}}^{\mathrm{m}}/\rho_{\mathrm{H_2O}}$ the superficial velocity of water through PEM. Considering that the ethanol at the cathode was from the anode due to crossover and then it was oxidized and vaporized, obviously the ethanol concentration at the cathode is much less than that at the anode. Thus, $C_{\mathrm{EtOH}}^{\mathrm{cath}}$ can be omitted. Consequently, Eq. (22) is reduced into Eq. (23):

$$N_{\mathrm{EtOH}}^{\mathrm{m}} = \frac{C_{\mathrm{EtOH}}^{\mathrm{an}} \mathrm{e}^{v^{\mathrm{m}}/k^{\mathrm{m}}}}{\mathrm{e}^{v^{\mathrm{m}}/k^{\mathrm{m}}}} v^{\mathrm{m}} \tag{23}$$

This equation describes the ethanol transportation through PEM, which is known as ethanol crossover and it will be further examined.

Furthermore, the following equations, which describe the anode, cathode and overall reactions for a DEFC were also taken into account, while developing the mathematical model for the anode of a DEFC.

$$\text{Anode reaction}: \quad \mathrm{CH_3CH_2OH} + 3\mathrm{H_2O} \rightarrow 2\mathrm{CO_2} + 12\mathrm{H^+} + 12\mathrm{e^-} \tag{24}$$

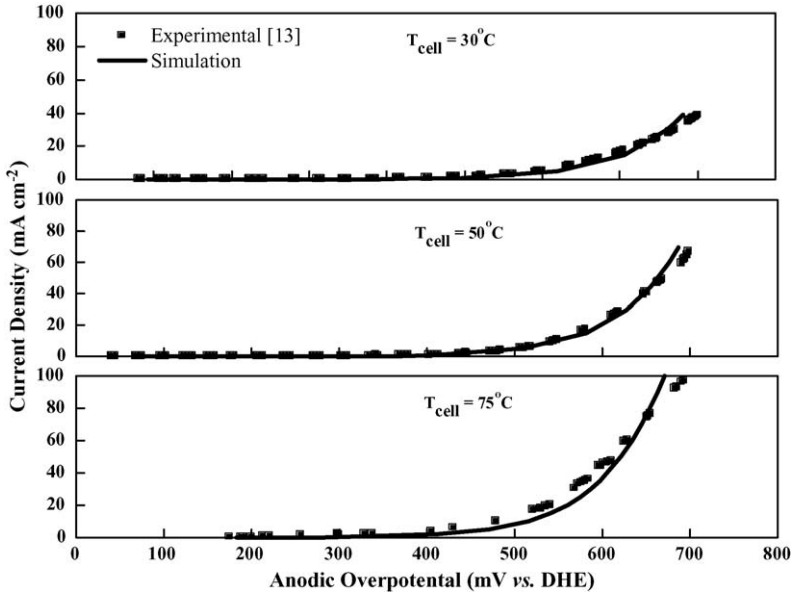

Fig. 2. Anode polarization curves of a DEFC of the experimental [13] and simulation results.

$$\text{Cathode reaction}: \quad 3O_2 + 12H^+ + 12e^- \rightarrow 6H_2O \tag{25}$$

$$\text{Overall reaction}: \quad CH_3CH_2OH + 3O_2 \rightarrow 2CO_2 + 3H_2O \tag{26}$$

3. Results and discussion

3.1. Anode polarization curves of a DEFC

Fig. 2 gives the comparison between the calculated anode overpotential using the present mathematical model and the experimental results [13]. The anode polarization was obtained by scanning the potential with the anode (PtRu/C was the catalyst) supplied with 1.0 M ethanol aqueous solution as the working electrode and the cathode fed by 1 atm humidified hydrogen serving both as the counter electrode and the *dynamic hydrogen reference electrode* (DHE). The operation conditions have been reported in detail previously [13]. As it can be seen from Fig. 2 there is a good agreement between the experimental and simulation results. This suggests that the present model can work very well. It should be noted that the parameters used in the present model were deduced from the experimental results [10] and they are shown in Table 1.

Table 1
Parameters used for modeling from the experimental results [10]

T (°C)	I_o (mA)	α_a	A_v (cm^2)	γ
30	0.34805	0.0285	5.0	0.25
50	0.39917	0.0365	5.0	0.25
75	0.68331	0.040	5.0	0.25

3.2. Effect of the catalyst layer thickness on the anode overpotential

Fig. 3 shows the effect of the catalyst layer thickness on the anode overpotential. In Fig. 3(a), the effect of the catalyst layer

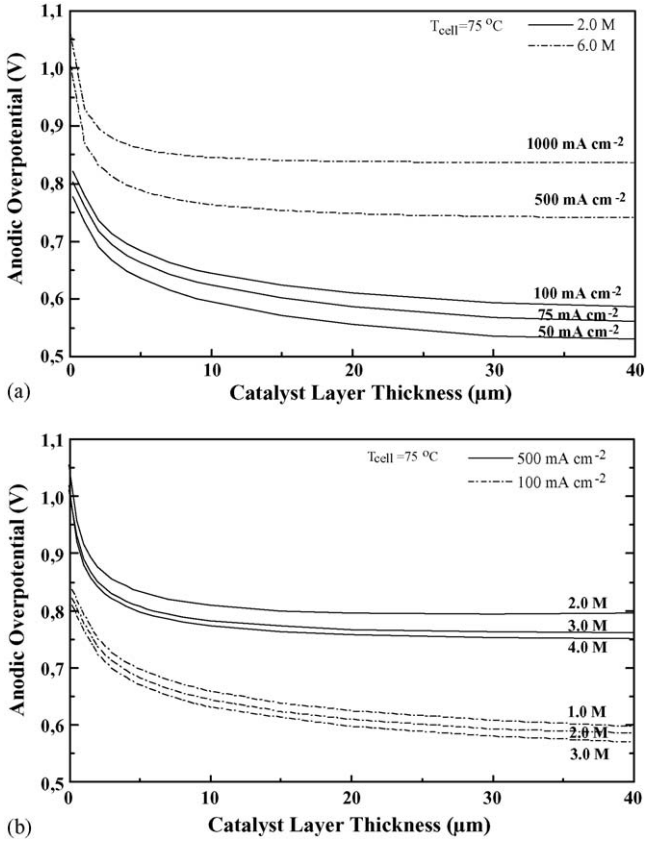

Fig. 3. Effect of the catalyst layer thickness on the anode overpotential at different current densities (a) and different ethanol feed concentrations (b).

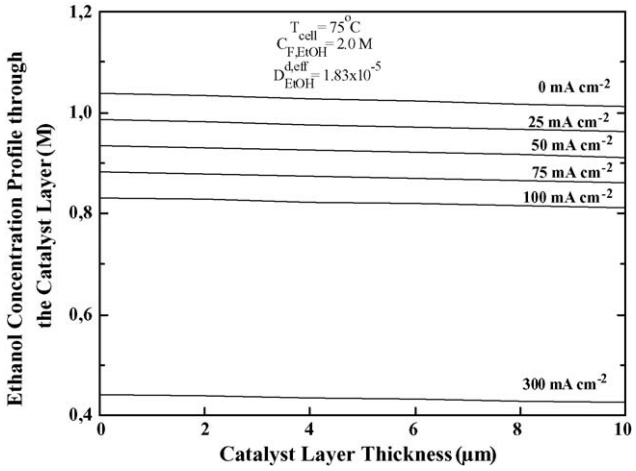

Fig. 4. Effect of the catalyst layer thickness on the ethanol concentration profile through the catalyst layer, $C_{F,EtOH} = 2$ M, $T_{cell} = 75\,^{\circ}C$.

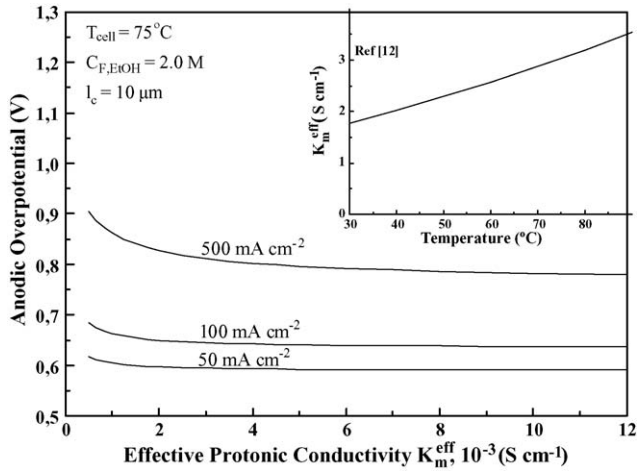

Fig. 5. Dependence of the anode overpotential on the effective protonic conductivity at different current densities, $T_{cell} = 75\,^{\circ}C$. The inset shows the dependence of K_m^{eff} on the temperature.

thickness on the anode overpotential at different current densities is presented. Two different ethanol feed concentrations were considered in order to obtain results in a wide range of current densities. Fig. 3(b) illustrates the effect of the catalyst layer thickness on the anode overpotential for different ethanol feed concentrations. As one can observe when the catalyst layer thickness is up to 10 μm, the anode overpotential decreases sharply. This could be due to the insufficient catalyst surface and thus leading to the activation loss [12]. Above this thickness value, the overpotential continues to decrease, but slowly, up to a certain level and then it keeps almost constant in all the investigated current densities ranging from 50 to 1000 mA cm^{-2}. More specifically in Fig. 3(a), under the considered operation conditions: $I = 100$ mA cm^{-2}, $C_{F,EtOH} = 2.0$ M and $T_{cell} = 75\,^{\circ}C$, the anode overpotential decreases from 0.645 to 0.610 V as the catalyst layer thickness increases from 10 to 20 μm. Moreover for the same thickness change, at $I = 1000$ mA cm^{-2}, $C_{F,EtOH} = 6.0$ M and $T_{cell} = 75\,^{\circ}C$, the overpotential decreases from 0.851 to 0.849 V. Considering this, the value of 10 μm for the catalyst layer thickness was used in the following calculations.

The effect of the catalyst layer thickness on the ethanol concentration profile through the catalyst layer is given in Fig. 4. The predicted ethanol concentration through the catalyst layer at different current densities is presented. It can be distinguished that as the current density increases, the predicted ethanol concentration profile in the catalyst layer is slightly and linearly decreased. It is worthy to notice that in the case of 0 mA cm^{-2}, despite that the ethanol feed concentration was 2.0 M, at the diffusion layer/catalyst layer interface the ethanol concentration is only 1.04 M. This value is affected mostly by the mass transfer coefficient (k_g) and less by the effective diffusion coefficient of ethanol in the diffusion layer ($D_{EtOH}^{d,eff}$).

3.3. Effect of the effective protonic conductivity K_m^{eff} on the anode overpotential

Fig. 5 illustrates the dependence of the anode overpotential on the effective protonic conductivity at constant operating temperature (75 °C). In the inset of Fig. 5, the change of K_m^{eff} along with the temperature is also shown. As expected, the anode overpotential decreases if the catalyst layer possesses better protonic conductivity. For example, at 100 mA cm^{-2}, when the protonic coefficient in the catalyst layer increases from 1×10^{-3} to 3.2×10^{-3} S cm^{-1}, the corresponding anode overpotential decreases from 0.667 to 0.648 V. Increasing the protonic coefficient up to 1×10^{-2} S cm^{-1}, the anode overpotential further decreases up to 0.641 V. At higher current density values, the corresponding decrement for the anode overpotential is even higher. Obviously, based on the above information, the decreased overpotential can be achieved by increasing the protonic conductivity of the catalyst layer. This suggests that, in order to increase the effective protonic conductivity in the catalyst layer, the void volume in the catalyst layer (the space among catalyst particles) should be filled to a large extent with ionomer [12]. From the inset of Fig. 5, it can be clearly seen that the effective protonic conductivity is affected by the temperature and it increases as the temperature increases. It is worthy to note that the effect of the effective diffusion coefficient on the anode overpotential was also investigated and it was found that it had almost no effect on the anode overpotential (Table 2).

3.4. Parameters influencing ethanol crossover rate

In Fig. 6 the effect of the current density on the ethanol crossover rate at different operating temperatures is presented. As it can be seen the increase of the current density affects the ethanol crossover rate in two conflicting ways. From one side, one will expect that increasing the current density would definitely result in a decrement of the ethanol crossover, due to the fact that more ethanol will participate in the electrochemical reaction, thus decreasing the concentration difference between the two sides of PEM. However, when high ethanol feed concentrations (i.e. 4.0 M) are used, a volcano behavior is presented as shown in Fig. 6. This could be explained by the fact that the total ethanol crossover rate is the combined result of the diffu-

Table 2
Basic parameter values

Parameter	Value	Ref.
Anode transfer coefficient, α_a at 75 °C	0.04	[13]
Electrode surface (cm^2)	5	
Reference exchange current density, i_o	0.68331	[13]
Order of reaction	0.25	[13]
Catalyst layer thickness, t_c (μm)	10	
Diffusion layer thickness, t_d (μm)	30	
PEM thickness, t_m (μm)	15	
Reference ethanol concentration (M)	0.5	[13]
Void fraction of catalyst layer, ε^c	0.32	
Diffusion coefficient of ethanol in water, $D_{d,EtOH}$ ($cm^2\ s^{-1}$) at 75 °C	1.83×10^{-5}	[27]
Diffusion coefficient of ethanol in PEM, D^m_{EtOH} ($cm^2\ s^{-1}$) at 75 °C	4.1×10^{-5}	[28]
Void fraction of diffusion layer, ε^d	0.8	
Protonic conductivity of the ionomer, K_m ($S\ cm^{-1}$)	0.1416	[12]
Effective protonic conductivity in catalyst layer, K^{eff}_m ($S\ cm^{-1}$)	3.2×10^{-3}	
Electronic conductivity of solid phase (Pt–C), K_s ($S\ cm^{-1}$)	8.13×10^{-6}	[22]
Effective conductivity of solid phase in catalyst layer, K^{eff}_s ($S\ cm^{-1}$)	3.78×10^{-6}	
Volume fraction of ionomer phase in catalyst layer, ε^c_m	0.04	
Electro-osmotic drag coefficient of water, λ_{H_2O}	3.16	[12]
Volume fraction of solid phase (Pt–C) in catalyst layer, ε^c_s	0.6	
Ethanol feed concentration $C_{F,EtOH}$ (M)	1.0	

sion, due to the concentration difference between the anode and the cathode and the electro-osmotic drag. As the current density increases, the difference in ethanol concentration between anode and cathode is definitely reduced since more ethanol is involved in the ethanol electro-oxidation at the anode. On the other hand, the electro-osmotic drag increases due to the fact that more protons are transported through the membrane, which leads to more ethanol molecules permeated to the cathode. The resultant effect of these two phenomena can give a reasonable explanation for the observed results. At lower temperatures (<75 °C) such as 30 and 50 °C, this volcano behavior of the ethanol crossover rate along with the current density is more obvious. This is probably due to the lower diffusion coefficient of ethanol in both diffusion layer and PEM. Similar predictions have been obtained concerning the anode behavior of a direct methanol fuel cell [12].

Fig. 7 shows the effect of the temperature on the ethanol crossover rate at different current densities and different ethanol feed concentrations. It can be observed that ethanol crossover rate is increased with the temperature increment as expected due to the increased kinetics at higher temperature. From Fig. 7(a) it can be seen that the current density affects the ethanol crossover rate especially at high current densities. Moreover, the activation energies are higher at high current densities. This could be attributed to the fact that as the current density increases, the electro-osmotic drag is increased simultaneously because more protons will be transported through PEM. The effect of the ethanol feed concentration on the ethanol crossover rate, at different operation temperature is presented in Fig. 7(b). From the parallel lines, it is clear that the ethanol feed concentration does not affect the apparent activation energy of ethanol crossover in the investigated range.

Fig. 8 illustrates the effect of the ethanol feed concentration on the ethanol crossover rate at different current densities. The ethanol crossover rate increases linearly with the increment of the ethanol feed concentration. In the case of $C_{F,EtOH} = 3.0$ M, there is a point where the first three values of the current density are intersected. This could be explained by the volcano behavior of the ethanol crossover rate along with the current density as observed in Fig. 6.

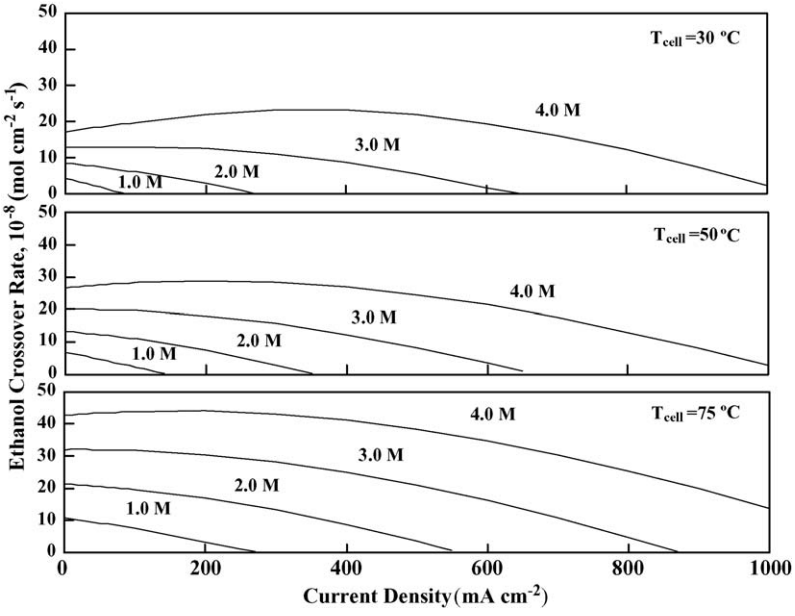

Fig. 6. Effect of the current density on the ethanol crossover rate at different temperatures and different ethanol concentrations.

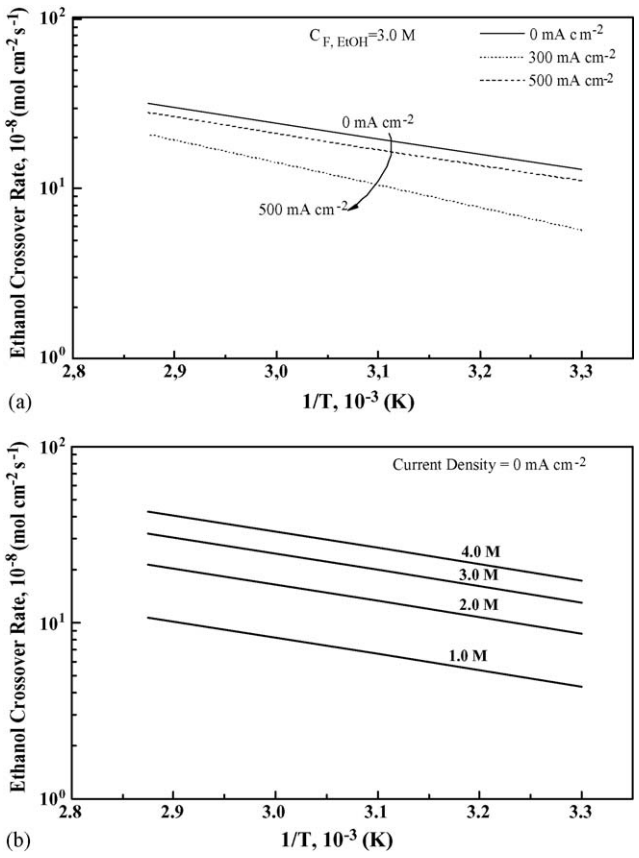

Fig. 7. Effect of temperature on ethanol crossover rate at different current densities (a) and different ethanol concentrations (b).

3.5. Simulation versus experimental results

A comparison between the simulation and experimental results, concerning ethanol crossover rate, is illustrated in Fig. 9. The effect of the ethanol feed concentration on the ethanol crossover rate at different operating temperatures, is shown in Fig. 9(a). It should be pointed out that the ethanol feed concentration that was taken into account in the present results was

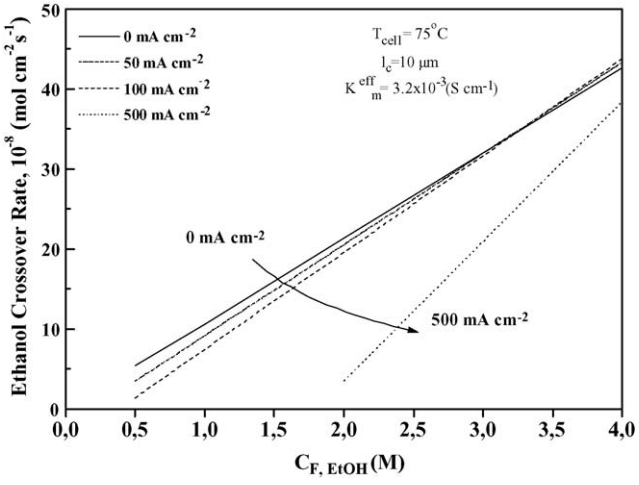

Fig. 8. Effect of the ethanol feed concentration on the ethanol crossover rate at different current densities. $T_{cell} = 75\,^{\circ}C$.

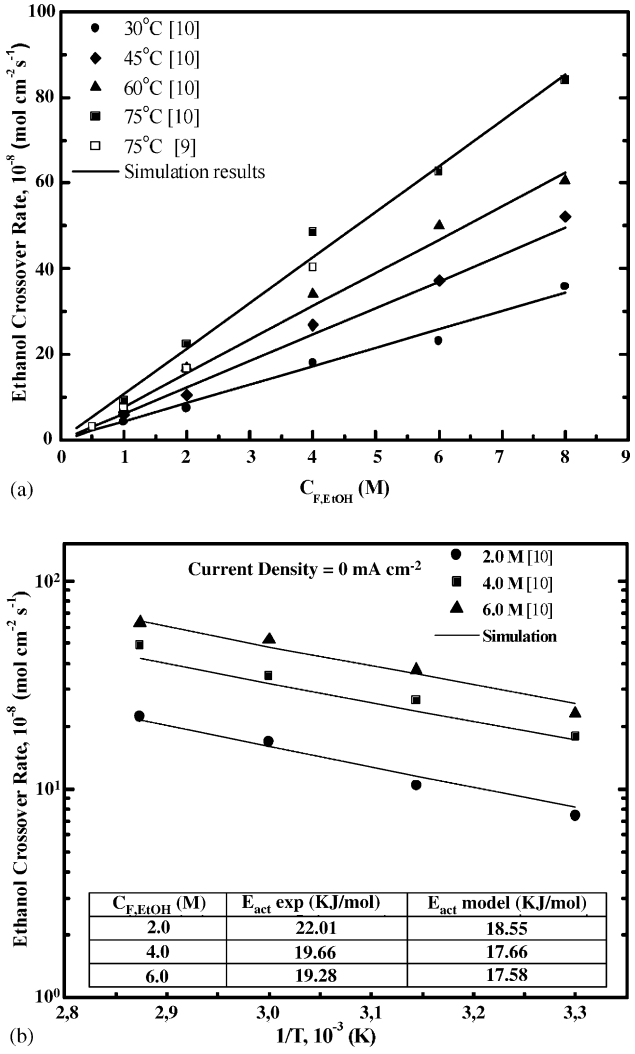

Fig. 9. (a and b) Comparison of the effect of ethanol feed concentration on ethanol crossover rate at $I = 0\,mA\,cm^{-2}$ between the experimental [9,10] and simulation results.

only up to 8.0 M. There are more experimental results concerning ethanol crossover rate at higher ethanol feed concentrations, which will be reported in our future work [10]. The effect of the operating temperature on the ethanol crossover rate along with the ethanol concentration is presented in Fig. 9(b). From the table shown in the inset of Fig. 9(b), it is obvious that there is almost the same apparent activation energy for all the investigated ethanol concentrations, as shown in Fig. 7(b). Finally, as it can be seen, there is a good agreement between the experimental and simulation results, which further indicates the validation of the present model.

4. Conclusions

In the present study, a mathematical model is developed in order to describe and predict the behavior of the anode of a direct ethanol proton exchange membrane fuel cell. The good agreement between the simulated and experimental results indicated that the present developed model could work very well. Based on the simulation results, it can be found that the increase of the

catalyst layer thickness and the effective protonic conductivity in the catalyst layer can contribute to the decrease in the anode overpotential. On the other hand, the optimal thickness of the catalyst layer is 10 μm considering from both performance and the cost point of view. It can also be found that the ethanol feed concentration, the operation temperature and the current density are the main parameters affecting ethanol crossover rate from the anode to the cathode through the electrolyte membrane.

Acknowledgement

The authors would like to thank the "Pythagoras 2004" programme from the Greek Ministry of National Education and Religious Affairs for funding.

References

[1] W. Vielstich, A. Lamm, H.A. Gasteiger, Handbook of Fuel Cells, Fundamentals Technology and Applications, vol. 1–4, John Wiley, 2003.
[2] J. Wang, S. Wasmus, R.F. Savinell, J. Electrochem. Soc. 142 (1995) 4218.
[3] K. Haraldsson, K. Wipke, J. Power Sources 126 (2004) 88.
[4] S. Song, W. Zhou, J. Tian, R. Cai, G. Sun, Q. Xin, S. Kontou, P. Tsiakaras, J. Power Sources 145 (2005) 266.
[5] S.Q. Song, W.J. Zhou, Z.H. Zhou, L.H. Jiang, G.Q. Sun, Q. Xin, V. Leontidis, S. Kontou, P. Tsiakaras, Int. J. Hydrogen Energy 30 (2005) 995.
[6] W.J. Zhou, S.Q. Song, W.Z. Li, Z.H. Zhou, G.Q. Sun, Q. Xin, S. Douvartzides, P. Tsiakaras, J. Power Sources 140 (2005) 50.
[7] S. Song, G. Wang, W. Zhou, X. Zhao, G. Sun, Q. Xin, S. Kontou, P. Tsiakaras, J. Power Sources 140 (2005) 103.
[8] J. Kim, S.M. Lee, S. Srinivasan, J. Electrochem. Soc. 142 (1995) 2670.
[9] S. Song, W. Zhou, Z. Liang, R. Cai, G. Sun, Q. Xin, V. Stergiopoulos, P. Tsiakaras, Appl. Catal. B: Environ. 55 (2005) 65.
[10] S. Kontou, N. Kaklidis, I. Koutla, S. Song, P. Tsiakaras, First European Fuel Cell Technology & Applications Conference, Rome, Italy, December 14–16, 2005.
[11] S. Song, P. Tsiakaras, Appl. Catal. B, in press.
[12] K.T. Jeng, C.W. Chen, J. Power Sources 112 (2002) 367.
[13] X. Zhao, G. Sun, L. Jiang, S. Yang, B. Yi, Chin. J. Catal. 25 (2004) 983.
[14] S. Song, S. Douvartzides, P. Tsiakaras, J. Power Sources 145 (2005) 495.
[15] W.J. Zhou, B. Zhou, W.Z. Li, Z.H. Zhou, S.Q. Song, G.Q. Sun, Q. Xin, S. Douvartzides, M. Goula, P. Tsiakaras, J. Power Sources 126 (2004) 16.
[16] V. Galvita, G. Semin, V. Belyaev, V. Semikolenov, P. Tsiakaras, V. Sobyanin, Appl. Catal. A 220 (2001) 123.
[17] W.J. Zhou, S.Q. Song, W.Z. Li, G.Q. Sun, Q. Xin, S. Kontou, K. Poulianitis, P. Tsiakaras, Solid State Ionics 175 (2004) 797.
[18] P. Tsiakaras, S. Douvartzides, A. Demin, V. Sobyanin, Solid State Ionics 152–153 (2002) 721.
[19] J.J. Baschuk, X. Li, J. Power Sources 86 (2000) 181.
[20] C.W. Tobias, Advances in Electrochemistry and Electrochemical Engineering, Wiley, New York, 1962, p. 19.
[21] W. Zhou, Z. Zhou, S. Song, W. Li, G. Sun, P. Tsiakaras, Q. Xin, Appl. Catal. B: Environ. 46 (2003) 273.
[22] S.F. Baxter, V.S. Battaglia, R.E. White, J. Electrochem. Soc. 146 (1999) 437.
[23] P.R. Pathapati, X. Xue, J. Tang, Renewable Energy 30 (2005) 1.
[24] R. Sousa, E.R. Gonzalez, J. Power Sources 147 (2005) 32.
[25] L. You, H. Liu, Int. J. Heat Mass Transfer 45 (2002) 2277.
[26] M. Mulder (Ed.), Basic Principles of Membrane Technology, second ed., Twente University, 1996.
[27] R.C. Reid, J.M. Prausnitz, B.E. Poling, The Properties of Gases & Liquids, fourth ed., Mc Graw-Hill International Editions, Chemical Engineering Series, 1988.
[28] S. Kato, K. Nagahama, H. Noritomi, H. Asai, J. Membr. Sci. 72 (1992) 31.